# Stress Distribution around Circular/Elliptical/ Triangular Holes in Infinite Composite Plate

Dharmendra S Sharma

*Abstract*— **General stress functions for determining the stress concentration around circular, elliptical and triangular cutouts in laminated composite infinite plate subjected to arbitrary biaxial loading at infinity are obtained using Muskhelishvili's complex variable method. The generalized stress functions are coded using MATLAB and the effect of fiber orientation, stacking sequence, loading factor, loading angle and cutout geometry on stress concentration around cutouts in orthotropic/anisotropic plates is studied. Some of the results are compared with existing literature and finite element solutions.**

*Index Terms* – **Composites, cutouts, failure criteria, stress concentration factors, stress functions**

## I. INTRODUCTION

Various shaped cutouts are made in structures and machines to satisfy certain service requirements. These cutouts work as stress raisers and may lead to catastrophic failure. The behavior of isotropic plates with such cutouts, under different loading conditions is already studied extensively by many researchers. But, the anisotropic media with various shaped discontinuity has received very little attention.

Using Kolosov-Muskhelishvili's [1] complex variable approach, some problems of simply connected regions are solved by Savin [2],Lekhnitskii [3], Ukadgaonker and Rao [4],[5], Ukadgaonker and Kakhandki [6], Nageswara Rao et al [7], Daoust and Hoa [8], Rezaeepazhand and Jafari [9], Sharma [10] etc.

Savin [2] and Lekhnitskii [3] found stress concentrations around circular, elliptical, triangular and square holes, mainly in isotropic media. Though, Savin [2] used integro-differential approach and Lekhnitskii [3] used series approach to define the stress function, the final outcomes are same. The analytic solutions for stress analysis of infinite anisotropic plate with irregular holes are presented by Ukadgaonker and Rao [4],[5] and Ukadgaonker and Kakhandki [6]. They adopted Gao's [11] arbitrary biaxial loading condition to eliminate superposition of two uniaxial loading problem to obtain solution for biaxial loading problem. Ukadgaonker and Rao [5], Daoust and Hoa [8] and Sharma [10] presented solutions for stress distribution around triangular hole with blunt corners in composite plates, whereas Nageswara Rao et al [7] found stress field around square and rectangular holes. Ukadgaonker and Rao [5] and Daoust and Hoa [8] explained effect of corner bluntness, material parameters and fibre orientation on stress concentration factor. Rezaeepazhand and Jafari [9]

explained effect of load angle and hole orientation on maximum stress concentration factor for triangular, square and pentagonal hole with blunt corners, in isotropic media. The bluntness of the corner taken by them is significantly higher compared to Ukadgaonker and Rao [5] and Daoust and Hoa [8], and the outcome for triangular cutout in isotropic plate is in terms of comparatively smaller value of stress concentration.

In this paper, Kolosov-Mushkhelishvilli's complex variable approach is adopted to obtain generalized stress functions. The effect of hole geometry, material properties, fiber orientation, stacking sequence, loading factor and loading angle on stress field around cut-outs is studied. For numerical results Graphite/epoxy, Glass/epoxy and isotropic materials are considered.

## II. COMPLEX VARIABLE FORMULATION

A thin anisotropic plate is considered under generalized plane stress condition (Refer Fig. 1). The plate is assumed to be loaded in such a way that resultants lies in XOY plane. The mean values of strains along thickness of the plate can be represented by generalized Hooke's law.

$$\begin{Bmatrix} \varepsilon_x \\ \varepsilon_y \\ \gamma_{xy} \end{Bmatrix} = \begin{bmatrix} a_{11} & a_{12} & a_{16} \\ a_{12} & a_{22} & a_{26} \\ a_{16} & a_{26} & a_{66} \end{bmatrix} \begin{Bmatrix} \sigma_x \\ \sigma_y \\ \tau_{xy} \end{Bmatrix} \qquad (1)$$

Where,

$\sigma_x, \sigma_y, \tau_{xy}$ =mean value of stresses along thickness,

$a_{ij}$ =compliance co-efficient

In the absence of body forces the stress components can be written in terms of Airy's stress function (U) as follows:

$$\sigma_x = \frac{\partial^2 U}{\partial y^2} \; ; \; \sigma_y = \frac{\partial^2 U}{\partial x^2} \; ; \; \tau_{xy} = -\frac{\partial^2 U}{\partial x \partial y} \qquad (2)$$

Substituting equation (1) and equation (2) in strain-displacement compatibility condition

$$\frac{\partial^2 \varepsilon_x}{\partial y^2} + \frac{\partial^2 \varepsilon_y}{\partial x^2} = \frac{\partial^2 \gamma_{xy}}{\partial x \partial y} \text{ , we get}$$

$$\left.\begin{Bmatrix} a_{22}\dfrac{\partial^4 U}{\partial x^4} - 2a_{26}\dfrac{\partial^4 U}{\partial x^3 \partial y} \\ + (2a_{12}+a_{66})\dfrac{\partial^4 U}{\partial x^2 \partial y^2} \\ - 2a_{16}\dfrac{\partial^4 U}{\partial x \partial y^3} + a_{11}\dfrac{\partial^4 U}{\partial y^4} \end{Bmatrix}\right\} = 0 \qquad (3)$$

Dharmendra Sharma is with the Institute of Technology, Nirma University, Ahmedabad-382481, India (phone +91-2717-241911, ext 543 fax 91-2717-241911; email:dss_iit@yahoo.com )

Symbolically, the above equation can be written in terms of four linear differential operators as

$$D_1 D_2 D_3 D_4 U = 0 \qquad (4)$$

$$D_k (k = 1,2,3,4) = \frac{\partial}{\partial y} - s_k \frac{\partial}{\partial x},$$

Where, $s_k (k = 1,2,3,4)$ are the roots of the characteristic equation

$$\begin{pmatrix} a_{11}s^4 - 2a_{16}s^3 + (2a_{12} + a_{66})s^2 \\ - 2a_{26}s + a_{22} \end{pmatrix} = 0 \qquad (5)$$

The roots of equation (5) can be written as

$$s_1 = \alpha_1 + i\beta_1$$
$$s_2 = \alpha_2 + i\beta_2$$
$$s_3 = \alpha_1 - i\beta_1$$
$$s_4 = \alpha_2 - i\beta_2 \qquad (6)$$

On integrating equation (3), the Airy's stress function $U(x, y)$ can be represented as

$$U(x,y) = \begin{pmatrix} F_1(x + s_1 y) + F_2(x + s_2 y) \\ + F_3(x + s_3 y) + F_4(x + s_4 y) \end{pmatrix}$$

$$U(x,y) = \begin{pmatrix} F_1(z_1) + F_2(z_2) \\ + \overline{F_1(z_1)} + \overline{F_2(z_2)} \end{pmatrix} \qquad (7)$$

The analytic functions $\Phi(z_1)$, $\psi(z_2)$ and their conjugates are given by

$$\frac{dF_1}{dz_1} = \phi(z_1) ; \frac{dF_2}{dz_2} = \psi(z_2) ;$$

$$\frac{d\overline{F_1}}{d\overline{z_1}} = \overline{\phi(z_1)} ; \frac{d\overline{F_2}}{d\overline{z_1}} = \overline{\psi(z_2)} \qquad (8)$$

By substituting analytic functions from equation (8) into equation (7), and finally equation (7) into equation (2), the stress components in terms of $\phi(z_1)$ and $\psi(z_2)$ can be represented as

$$\sigma_x = 2\operatorname{Re}\left[s_1^2 \phi'(z_1) + s_2^2 \psi'(z_2)\right]$$

$$\sigma_y = 2\operatorname{Re}\left[\phi'(z_1) + \psi'(z_2)\right] \qquad (9)$$

$$\tau_{xy} = -2\operatorname{Re}\left[s_1 \phi'(z_1) + s_2 \psi'(z_2)\right]$$

The stresses in Cartesian coordinates given in equation (9) can be written in orthogonal curvilinear coordinate system by means of the following relations

$$\begin{Bmatrix} \sigma_\theta \\ \sigma_\rho \\ \tau_{\rho\theta} \end{Bmatrix} = \begin{bmatrix} m^2 & n^2 & 2mn \\ n^2 & m^2 & -2mn \\ -mn & mn & m^2 - n^2 \end{bmatrix} \begin{Bmatrix} \sigma_x \\ \sigma_y \\ \tau_{xy} \end{Bmatrix} \qquad (10)$$

m and n are the direction cosines.

### III. MAPPING FUNCTION

The area external to a given hole (here, circular, elliptical or triangular), in Z-plane is mapped conformably to the area outside the unit circle in ζ plane using following mapping function.

$$z = \omega(\zeta) = R\left[\left(\zeta + \sum_{k=1}^{N} \frac{m_k}{\zeta^k}\right)\right] \qquad (11)$$

R = Hole size constant

$\zeta = \rho e^{i\theta}$ (Here, $\rho$ =1 for unit circle)

$m_k = 0$, for circular hole

$k = 1, m_k = \left(\dfrac{a-b}{a+b}\right)$, for elliptical hole, where, $a$ and $b$ are the semi major and semi minor axis of the ellipse, respectively

$k = 3,5,8,11,14,17...$ and $m_3 = 1/3$; $m_5 = 1/45$; $m_8 = 1/162$; $m_{11} = 7/2673$; $m_{14} = 1/729$; $m_{17} = 91/111537$, for triangular hole.

For anisotropic materials, the deformations undergo affine transformation. Hence, the mapping function (Equation (11)) is modified by introducing complex parameters $s_j$.

$$z_j = \omega_j(\zeta) = \frac{R}{2}\left[a_j\left(\frac{1}{\zeta} + \sum_{k=1}^{N} m_k \zeta^k\right) + b_j\left(\zeta + \sum_{k=1}^{N} \frac{m_k}{\zeta^k}\right)\right]$$

$$a_j = (1 + is_j), b_j = (1 - is_j) ; \quad j=1,2. \qquad (12)$$

### IV. ARBITRARY BIAXIAL LOADING CONDITIONS

In order to consider several cases of in-plane loads, the arbitrary biaxial loading condition is introduced into the boundary conditions. This condition has been adopted from Gao's [10] solution for elliptical hole in isotropic plate. By means of this condition solutions for biaxial loading can be obtained without the need of superposition of the solutions of the uni-axial loading. This is achieved by introducing the biaxial loading factor λ and the orientation angle β into the boundary conditions at infinity.

The boundary conditions for in-plane biaxial loading conditions are as follows:

$$\sigma_{x'}^{\infty} = \lambda\sigma; \quad \sigma_{y'}^{\infty} = \sigma; \quad \tau_{x'y'}^{\infty} = 0 \quad \text{at } |z| \to \infty$$

Where, $\sigma_{x'}^{\infty}$ and $\sigma_{y'}^{\infty}$ are stresses applied about x`, y` axes at infinity (Refer Fig. (1)). By applying stress invariance into above boundary conditions, boundary conditions about XOY can be written explicitly as:

$$\sigma_x = \frac{p}{2}[(\lambda + 1) + (\lambda - 1)\cos 2\beta]$$

$$\sigma_y = \frac{p}{2}[(\lambda + 1) - (\lambda - 1)\cos 2\beta]$$

$$\tau_{xy} = \frac{p}{2}[(\lambda - 1)\sin 2\beta] \qquad (13)$$

For inclined uni-axial tension: λ=0, β≠0
(a) Loading along x-axis     : λ=0, β=π/2
(b) Loading along y-axis     : λ=0, β=0
For equi-biaxial tension     : λ=1, β=0
For shear stress     : λ=-1, β=π/4 or 3π/4
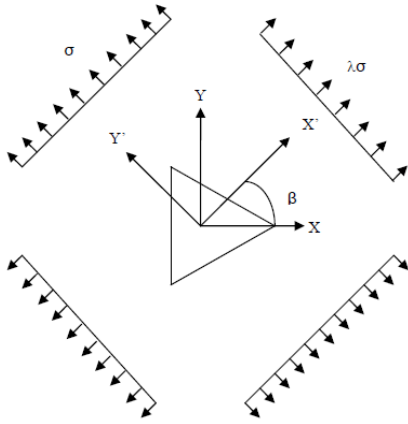


Fig. 1 Arbitrary biaxial loading condition

## V. STRESS FUNCTION FOR CUTOUTS OF DIFFERENT SHAPES

The scheme for solution of anisotropic plate containing a cutout subjected to remotely applied load is shown in Fig. (2). To determine the stress function, the solution is split into two stages:

*A. First Stage*

The stress functions, $\phi_1(z_1)$ and $\psi_1(z_2)$ are determined for the hole free plate under the application of remotely applied load. The boundary conditions $f_1$ and $f_2$ are found for the fictitious hole using stress functions $\phi_1(z_1)$ and $\psi_1(z_2)$.

The stress function $\phi(z_1)$ and $\psi(z_2)$ are obtained for hole free plate due to remotely applied load $\sigma_x^\infty, \sigma_y^\infty$ as

$$\phi_1(z_1) = B^* z_1$$
$$\psi_1(z_2) = (B'^* + iC'^*) z_2 \tag{14}$$

Where,

$$B^* = \frac{\sigma_x^\infty + (\alpha_2^2 + \beta_2^2)\sigma_y^\infty + 2\alpha_2\tau_{xy}^\infty}{2((\alpha_2 - \alpha_1)^2 + (\beta_2^2 - \beta_1^2))}$$

$$B'^* = \frac{(\alpha_1^2 - \beta_1^2 - 2\alpha_1\alpha_2)\sigma_y^\infty - \sigma_x^\infty - 2\alpha_2\tau_{xy}^\infty}{2((\alpha_2 - \alpha_1)^2 + (\beta_2^2 - \beta_1^2))}$$

$$C'^* = \frac{\begin{pmatrix} [(\alpha_1 - \alpha_2)]\sigma_x^\infty + [\alpha_2(\alpha_1^2 - \beta_1^2) \\ -\alpha_1(\alpha_2^2 - \beta_2^2)]\sigma_y^\infty \\ +[(\alpha_1^2 - \beta_1^2) - (\alpha_2^2 - \beta_2^2)]\tau_{xy}^\infty \end{pmatrix}}{2\beta_2[(\alpha_2 - \alpha_1)^2 + (\beta_2^2 - \beta_1^2)]}$$

C is taken zero, because no rotation is allowed.

The boundary conditions $f_1, f_2$ on the fictitious hole are determined from these stress functions as follows

$$f_1 = 2\operatorname{Re}[\phi_1(z_1) + \psi_1(z_2)]$$
$$f_2 = 2\operatorname{Re}[s_1\phi_1(z_1) + s_2\psi_1(z_2)] \tag{15}$$

'Re' real part of complex number.

By substituting equation (12) into equation (14), and finally equation (14) into equation (15), the boundary conditions are obtained as follows:

$$f_1 = \begin{bmatrix} (K_1 + \overline{K_2})\left(\dfrac{1}{\xi} + \sum_{k=1}^{N} m_k \xi^k\right) \\ + (K_2 + \overline{K_1})\left(\xi + \sum_{k=1}^{N} \dfrac{m_k}{\xi^k}\right) \end{bmatrix}$$

$$f_2 = \begin{bmatrix} (K_3 + \overline{K_4})\left(\dfrac{1}{\xi} + \sum_{k=1}^{N} m_k \xi^k\right) \\ + (K_4 + \overline{K_3})\left(\xi + \sum_{k=1}^{N} \dfrac{m_k}{\xi^k}\right) \end{bmatrix} \tag{16}$$

Where,

$$K_1 = \left(\frac{R}{2}\right)\left[B^* a_1 + (B'^* + iC'^*)a_2\right]$$

$$K_2 = \left(\frac{R}{2}\right)\left[B^* b_1 + (B'^* + iC'^*)b_2\right]$$

$$K_3 = \left(\frac{R}{2}\right)\left[s_1 B^* a_1 + s_2(B'^* + iC'^*)a_2\right]$$

$$K_4 = \left(\frac{R}{2}\right)\left[s_1 B^* b_1 + s_2(B'^* + iC'^*)b_2\right]$$

*B. Second Stage*

For the second stage solution, the stress functions $\phi_0(z_1)$ and $\psi_0(z_2)$ are determined by applying negative of the boundary conditions $f_1^0 = -f_1$ and $f_2^0 = -f_2$ on its hole boundary in the absence of the remote loading.

A. The stress functions ($\phi_1(z_1)$ and $\psi_1(z_2)$) for the hole free plate under the application of remotely applied load. The boundary conditions at the hole circumference is $f_1$ and $f_2$

B. The second stage stress functions ($\phi_0(z_1)$ and $\psi_0(z_2)$) for plate with hole, without load at infinity ($f^0_1 = -f_1$ and $f^0_2 = -f_2$)

C. The stress function ($\phi(z_1)$ and $\psi(z_2)$) for plate with hole, subjected to remotely applied load.
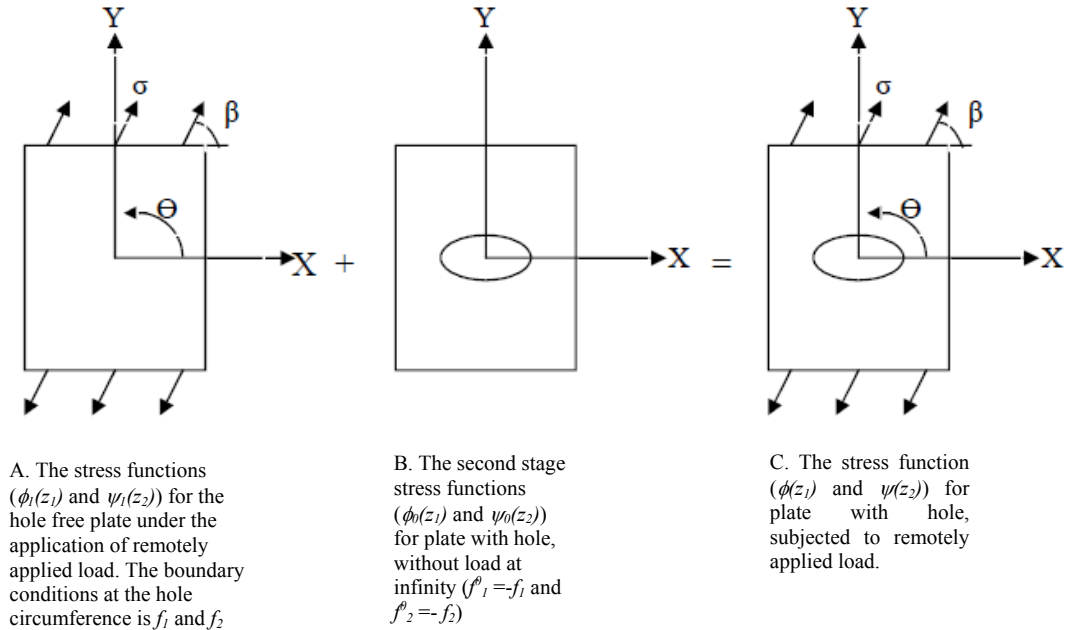
Fig.2. Problem configuration with scheme of solution

The stress functions of second stage solution are obtained using these new boundary conditions $(f_1^0, f_2^0)$ into Schwarz formula:

$$\phi_0(\zeta) = \frac{i}{4\pi(s_1 - s_2)} \int_\gamma (s_2 f_1^0 - f_2^0) \frac{t+\zeta}{t-\zeta} \frac{dt}{t} + \lambda_1 \qquad (17)$$

$$\psi_0(\zeta) = \frac{-i}{4\pi(s_1 - s_2)} \int_\gamma (s_1 f_1^0 - f_2^0) \frac{t+\zeta}{t-\zeta} \frac{dt}{t} + \lambda_2 \qquad (18)$$

Where $\gamma$ is the boundary of the unit circle in $\zeta$-plane, t is the value of $\zeta$ on hole boundary, $\lambda_1$ and $\lambda_2$ are imaginary constants which will have no contribution towards stress field.

By evaluating the integral the stress functions are obtained as

$$\phi_0(\xi) = \left\{ \frac{a_3}{\xi} + b_3 \sum_{k=1}^{N} \frac{m_k}{\xi^k} \right\}$$

$$\psi_0(\xi) = -\left\{ \frac{a_4}{\xi} + b_4 \sum_{k=1}^{N} \frac{m_k}{\xi^k} \right\} \qquad (19)$$

Where,

$$a_3 = \left\{ \frac{1}{s_1 - s_2} \right\} \left[ s_2(K_1 + \overline{K_2}) - (K_3 + \overline{K_4}) \right]$$

$$b_3 = \left\{ \frac{1}{s_1 - s_2} \right\} \left[ s_2(K_2 + \overline{K_1}) - (K_4 + \overline{K_3}) \right]$$

$$a_4 = \left\{ \frac{1}{s_1 - s_2} \right\} \left[ s_1(K_1 + \overline{K_2}) - (K_3 + \overline{K_4}) \right]$$

$$b_4 = \left\{ \frac{1}{s_1 - s_2} \right\} \left[ s_1(K_2 + \overline{K_1}) - (K_4 + \overline{K_3}) \right]$$

*C. Final Solution*

The stress function $\phi(z_1)$ and $\psi(z_2)$ for single hole problem, can be obtained by adding the stress functions of first and second stage.

$$\phi(z_1) = \phi_1(z_1) + \phi_0(z_1)$$

$$\psi(z_2) = \psi_1(z_2) + \psi_0(z_2) \qquad (20)$$

## VI. RESULTS AND DISCUSSION

The numerical results are obtained for Graphite/epoxy ($E_1$=181GPa, $E_2$=10.3GPa, $G_{12}$=7.17GPa and $\nu_{12}$=0.28) and Glass/epoxy ($E_1$=47.4GPa, $E_2$=16.2GPa, $G_{12}$=7.0GPa and $\nu_{12}$=0.26). Some of the results are obtained for isotropic plate (E=200GPa, G=80GPa and $\nu$=0.25) also for sake of comparison. The steps followed in computer implementation are as under:

1. Choose the value of biaxial load factor, $\lambda$ and load angle, $\beta$ for the type of loading.
2. Calculate the compliance co-efficient, $a_{ij}$ from generalized Hooke's Law
3. Calculate the value of complex parameters of anisotropy $s_1$ and $s_2$ from the characteristic equation (Equation 1). Some of the constants of anisotropy $s_1$ and $s_2$ are presented in Table 1.
4. Calculate the constants: $a_1$, $b_1$, $a_2$, $b_2$, B, B', C', $K_1$, $K_2$, $K_3$, $K_4$ etc.
5. Evaluate the stress functions and their derivatives.
6. Evaluate stresses.

The stress functions obtained above are the generalized solutions. Using these functions, stress distribution for

different loading conditions and material parameters can be obtained.

The following loading cases have been considered.

1.    Plate subjected to uni-axial tension at infinite distance.

2.    Plate subjected to biaxial tension at infinite distance.

The stress concentration around elliptical hole varies as ratio of lengths of major axis (2a) to minor axis (2a) varies. The circle (a/b=1) and crack (a/b=∞) are the special case of ellipse. As $(a-b)/(a+b)$ approaches unity, the stress concentration at the end of major axis of the ellipse tends to be infinite for all materials under consideration (Refer Fig.(3)). For isotropic material the stress concentration is found higher when uni-axial load is applied compared to equi-biaxial loading.

Table 1 Constants of anisotropy

| Fiber angle | Graphite/epoxy | | Glass/epoxy | |
|---|---|---|---|---|
| | $s_1$ | $s_2$ | $s_1$ | $s_2$ |
| 0 | -0.0000 + .8936i | 0 + 0.8566i | 0.0000 + 2.3960i | -0.00 + 0.7139i |
| 90 | -0.000 + 1.1674i | 0.000 + 0.2043i | -0.000 + 1.4007i | 0.000 + 0.4174i |
| 0/90 | -0.000 + 3.6403i | 0.000 + 0.2747i | -0.000 + 2.0142i | 0.000 + 0.4965i |
| 45/-45 | -0.8597 + 0.511i | 0.8597 + 0.511i | -0.6045 + 0.7966i | 0.6045 + 0.7966i |

The Fig.(4) shows distribution of normalized tangential stress ($\sigma_\theta/\sigma$) around circular hole in infinite plate subjected to uniaxial ($\lambda=0$) loading at infinity. For all material under consideration (Graphite/epoxy (0/90), Graphite/epoxy (45/-45) and Isotropic Steel) compressive zone is evident at around $90^0$ and $270^0$. The maximum value of $\sigma_\theta/\sigma$ for Graphite/epoxy (45/-45) is not found at $0^0$ and $180^0$ but at $35^0$, $145^0$, $215^0$ and $325^0$. Also the maximum value for Graphite/epoxy (45/-45) is found smaller in comparison to other material in consideration.

The stress distribution around circular hole in composite/isotropic plate subjected to equi-biaxial loading can be seen in Fig. (5). As expected, isotropic material shows equal intensity of stress concentration around hole under hydrostatic state of stress ($\lambda=1$). The anisotropy brings in change in magnitude of stress concentration and also location of it.

The normalized tangential stress ($\sigma_\theta/\sigma$) around elliptical hole (semi major axis (a)/semi minor axis (b)=2.0) in infinite plate subjected to uni-axial ($\lambda=0$) and equi-biaxial ($\lambda=1$) loading at infinity is shown in Fig. (6) and Fig. (7), respectively. In all cases under consideration, uni-axial loading produces higher stress concentration compared to equi-bixial loading.
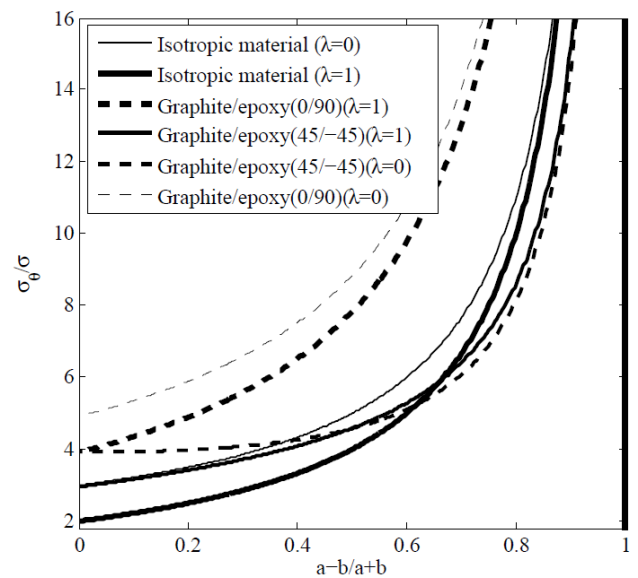


Fig. 3: Change in maximum stress concentration factor for elliptical hole as ratio $(a-b)/(a+b)$ varies from 0(crack) to 1.0(circle).
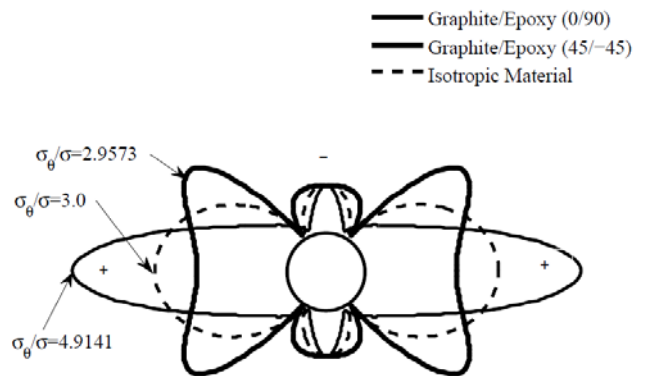


Fig. 4: The normalized tangential stress around circular hole in infinite plate subjected to uniaxial loading at infinity ($\lambda=0$)
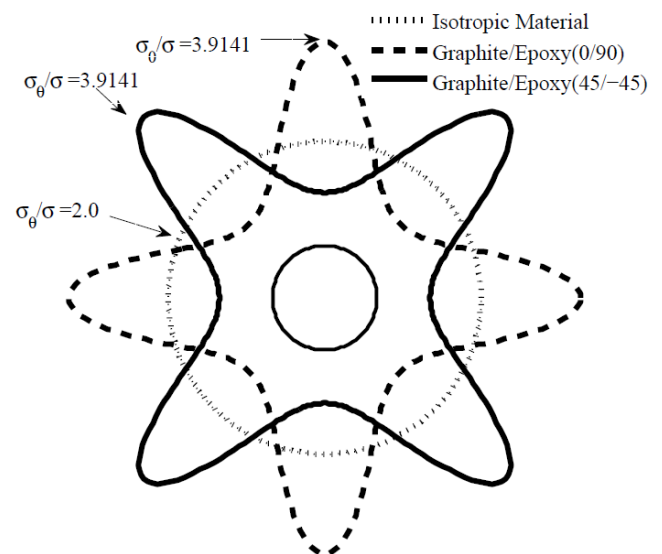


Fig. 5: The normalized tangential stress around circular hole in infinite plate subjected to equi-biaxial loading at infinity ($\lambda=1$)
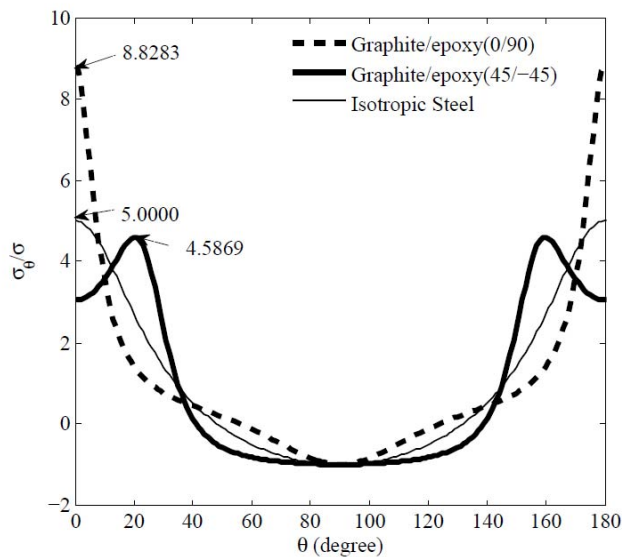
Fig. 6: The normalized tangential stress ($\sigma_\theta/\sigma$) around elliptical hole (a/b=2.0) in infinite plate subjected to uni-axial loading at infinity ($\lambda$=0)
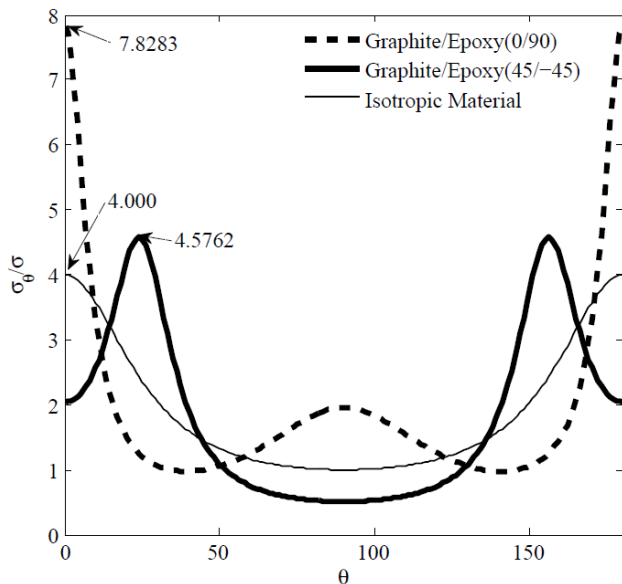


Fig. 7: The normalized tangential stress ($\sigma_\theta/\sigma$) around elliptical hole (a/b=2.0) in infinite plate subjected to equi-biaxial loading at infinity ($\lambda$=1)

The mapping function having 7 terms is used for triangular hole. As number of terms increases the hole shape converges to equilateral triangle and corner radius decreases (Refer Fig. (8)). With the 7-term mapping function the corner radius is found 0.0031 with side length 2.3676.

Stress is a point function and varies as we go around the hole boundary. Fig. (9) shows the stress distribution around triangular hole for different materials (corner radius, r=0.0476). The hole geometry and material parameters are taken same as Ukadgaonker and Rao [5] and Daoust and Hoa [8]. Fig. (9) can be compared with Fig. (3) (pp. 178) of Ukadgaonker and Rao [5] and Fig. (6) (pp. 127) of Daoust and Hoa [8].
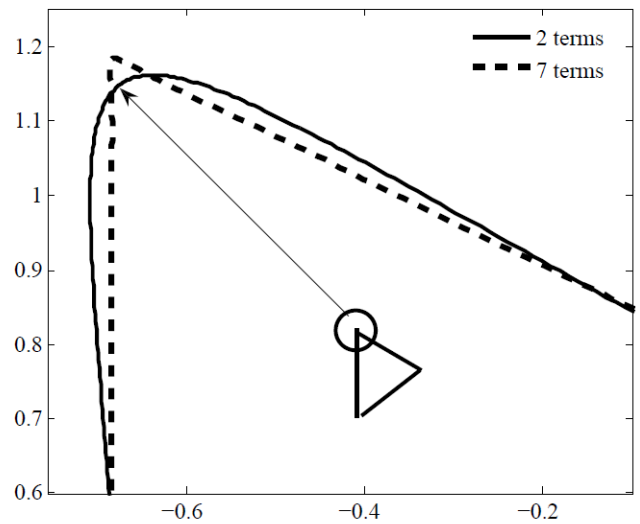


Fig. 8: Effect of number of terms on triangular hole shape
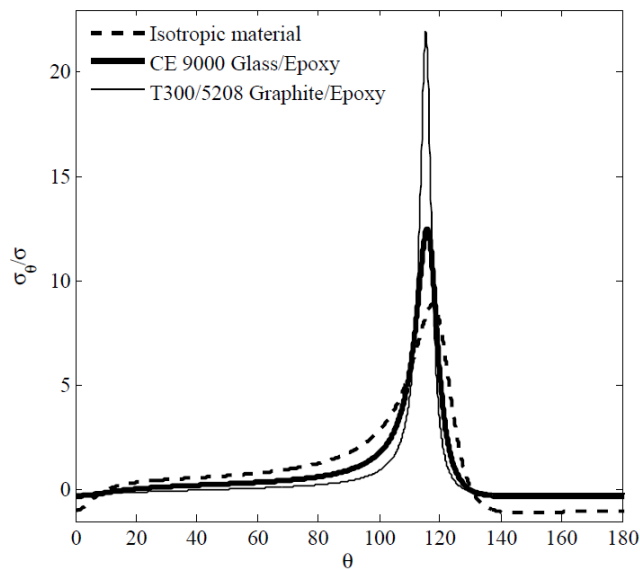


Fig. 9: Normalized tangential stress around the triangular hole (corner radius=0.0457, load angle, $\beta=0^0$, fiber orientation angle, $\Phi =0^0$).

The Graphite/epoxy and Glass/epoxy lamina are considered to understand the effect of fiber orientation angle on normalized tangential stress. The maximum ($\sigma_\theta/\sigma$) on the boundary of hole corresponding to fiber orientation angle ranging from $0^0$ to $90^0$ are shown in Fig. (10), (11) and (12). For plates with circular and elliptical hole the maximum tensile stress ($\sigma_\theta/\sigma$) increases as fiber orientation angle increases, whereas maximum compressive stress ($\sigma_\theta/\sigma$) decreases (Refer Fig. (10) and (11)). For the plate containing triangular hole the effect of fiber orientation angle ($\Phi$) on normalized tangential stress ($\sigma_\theta/\sigma$) for Graphite/epoxy and Glass/epoxy material is studied for load angle $\beta=0^0$ and $\beta=90^0$. The Graphite/epoxy plate subjected to uni-axial loading ($\lambda$=0, $\beta=0^0$) experience highest stress concentration when fiber orientation angle is $\Phi=90^0$. (Refer Fig. (12))
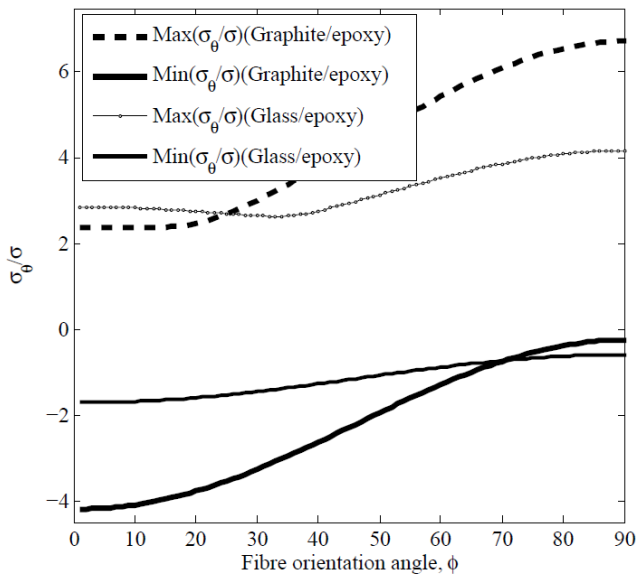
Fig. 10: Effect of fiber orientation angle ($\Phi$) on normalized tangential stress ($\sigma_\theta/\sigma$) for Graphite/epoxy and Glass/epoxy plate with circular hole



Fig. 12: Effect of fiber orientation angle ($\Phi$) on normalized tangential stress ($\sigma_\theta/\sigma$) for Graphite/epoxy and Glass/epoxy plate with triangular hole with corner radius=0.0031
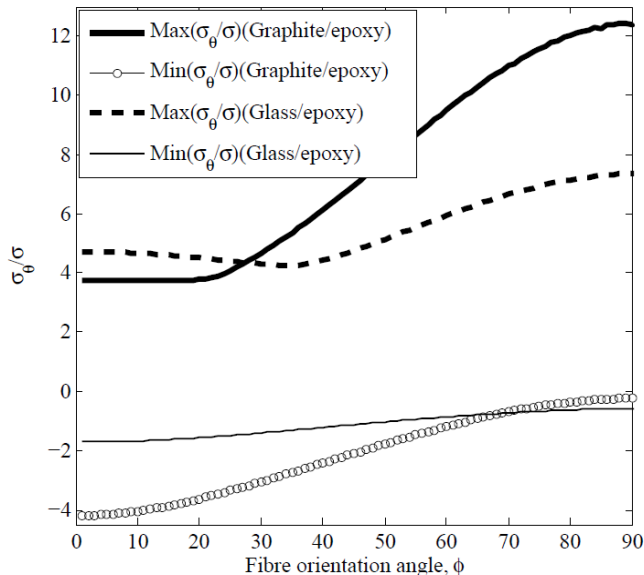


Fig. 11: Effect of fiber orientation angle ($\Phi$) on normalized tangential stress ($\sigma_\theta/\sigma$) for Graphite/epoxy and Glass/epoxy plate with elliptical hole having a/b=2.0
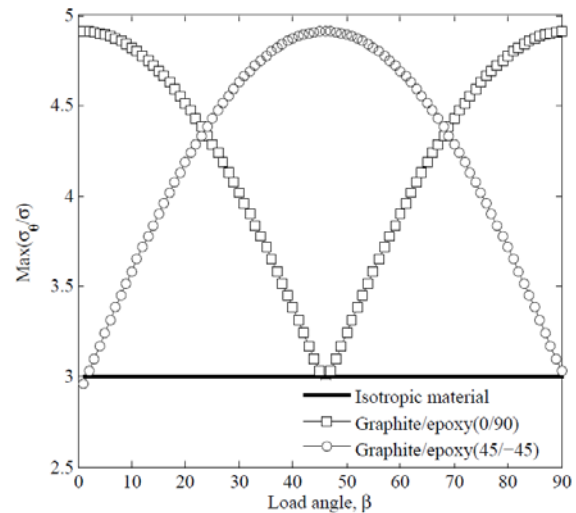


Fig. 13: Effect of load angle ($\beta$) on maximum normalized tangential stress ($\sigma_\theta/\sigma$) for Graphite/epoxy and isotropic plate with circular hole

The load angle ($\beta$) is varied from $0^0$ to $90^0$ and corresponding maximum normalized tangential stress is found. The effect of load angle ($\beta$) on maximum normalized tangential stress ($\sigma_\theta/\sigma$) for Graphite/epoxy and isotropic plate with circular, elliptical and triangular hole is presented in Fig. (13), (14) and (15), respectively. The maximum and minimum values of maximum normalized tangential stress corresponding to some load angle are tabulated in Table (2).

A comparison of von-Mises stresses for triangular hole having corner radius r=0.0031 unit for isotropic steel can be seen in Fig. (16). The results from present method ($\sigma_{von}/\sigma$=34.75) are in close confirmation with results obtained from finite element software (ANSYS) ($\sigma_{von}/\sigma$=34.09).

Table 2. The stress concentration factors for various load angles.

| | Graphite/ epoxy (0/90) | Graphite/ epoxy (45/-45) | Isotropic Material |
|---|---|---|---|
| Circular hole | 4.915 at $\beta=0^0$, $90^0$ | 4.9150 at $\beta=45^0$ | 3.0(For all load angle) |
| | 2.9578 at $\beta=45^0$ | 2.9578 at $\beta=0^0$, $90^0$ | |
| Elliptical hole (a/b=2) | 8.8301 at $\beta=90^0$ | 5.8502 at $\beta=63^0$ | 5.0 at $\beta=90^0$ |
| | 2.7621 at $\beta=33^0$ | 1.7798 at $\beta=0^0$ | 2.0 at $\beta=0^0$ |
| Triangular hole (r=0.0031) | 67.0607 at $\beta=90^0$ | 39.6906 at $\beta=29^0$ | 34.7472 at $\beta=30^0$, $90^0$ |
| | 28.6624 at $\beta=41^0$ | 22.7871 at $\beta=90^0$ | 25.8104 at $\beta=0^0$, $60^0$ |
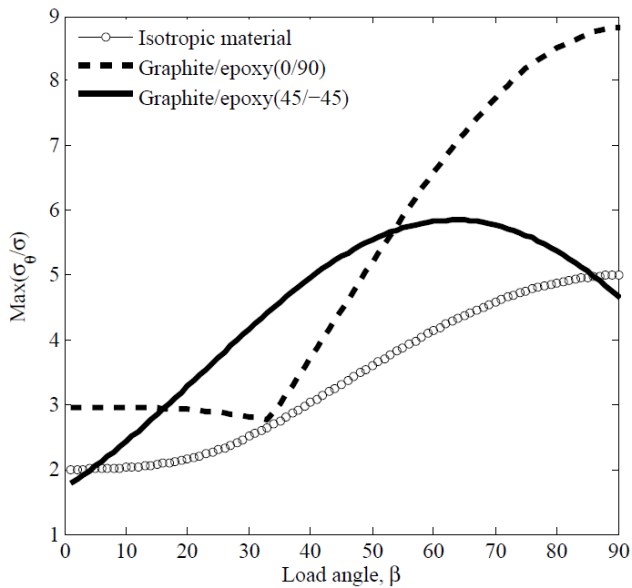
Fig. 14: Effect of load angle (β) on maximum normalized tangential stress ($\sigma_\theta/\sigma$) for Graphite/epoxy and isotropic plate with elliptical hole having a/b=2.0
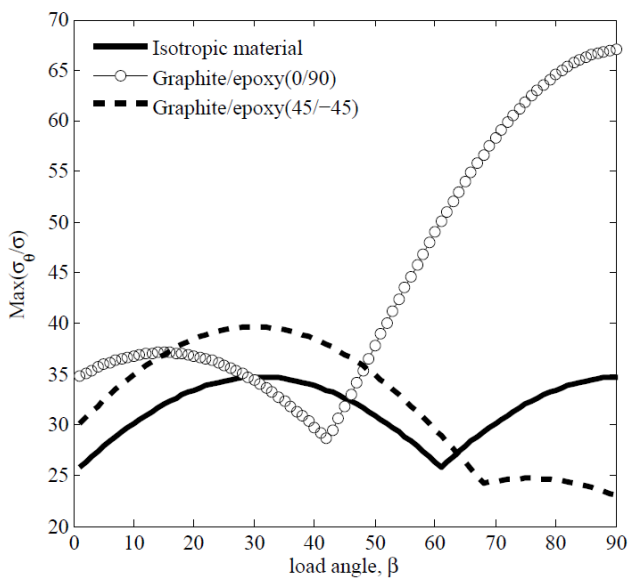


Fig. 15: Effect of load angle (β) on maximum normalized tangential stress ($\sigma_\theta/\sigma$) for Graphite/epoxy and isotropic plate with triangular having corner radius r=0.0031
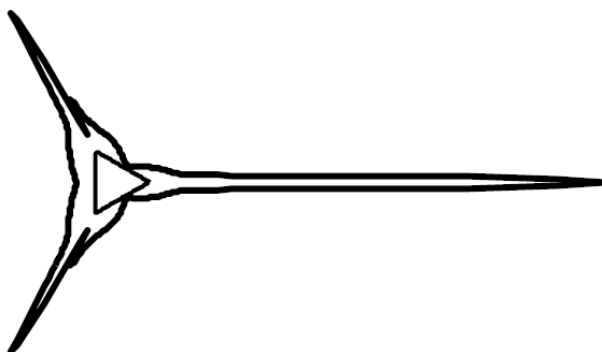


Fig. 16: von-Mises stress distribution around triangular hole (r=0.0031)

Table 2. The stress concentration factors for various load angles.

| | Graphite/ epoxy (0/90) | Graphite/ epoxy (45/-45) | Isotropic Material |
|---|---|---|---|
| Circular hole | 4.9150 at $\beta=0^0, 90^0$ | 4.9150 at $\beta=45^0$ | 3.0(For all load angle) |
| | 2.9578 at $\beta=45^0$ | 2.9578 at $\beta=0^0, 90^0$ | |
| Elliptical hole (a/b=2) | 8.8301 at $\beta=90^0$ | 5.8502 at $\beta=63^0$ | 5.0 at $\beta=90^0$ |
| | 2.7621 at $\beta=33^0$ | 1.7798 at $\beta=0^0$ | 2.0 at $\beta=0^0$ |
| Triangular hole (corner radius, r=0.0031) | 67.0607 at $\beta=90^0$ | 39.6906 at $\beta=29^0$ | 34.7472 at $\beta=30^0, 90^0$ |
| | 28.6624 at $\beta=41^0$ | 22.7871 at $\beta=90^0$ | 25.8104 at $\beta=0^0, 60^0$ |

VII. CONCLUSION

The general stress functions for determining the stress concentration around circular, elliptical and triangular cutouts in laminated composite plate subjected to arbitrary biaxial loading at infinity are obtained using Muskhelishvili's complex variable method. The solution presented here can be a handy tool for the designers. From the numerical results following points can be concluded:

1. The principle of superposition can be avoided by introducing biaxial loading factor.
2. As the ratio of minor to major axis in elliptical hole decreases from 1.0 to 0, the stress concentration approaches infinity. The stress concentration factor for isotropic material under biaxial loading is always smaller than that obtained when uniaxial loading is applied.
3. The stress field around hole is greatly affected by fiber orientation and stacking sequence of lamina. The magnitude and location of maximum stress around the hole periphery is highly dependent on fiber orientation and stacking sequence, for the given material and loading condition.
4. The stress concentration factor is greatly affected by material parameters and loading angle.
5. The bluntness of the corner radius has significant effect on stress concentration.

REFERENCES

[1] N. I. Muskhelishvili, *Some basic problems of the mathematical theory of elasticity*. Groningen-P.Noordhooff Ltd, 1963.
[2] G. N. Savin, *Stress concentration around holes*. New York-Pergamon Press, 1961.
[3] S. G. Lekhnitskii, *Theory of elasticity of an anisotropic elastic body*. San Francisco- Holden-Day Inc, 1963.

[4] V. G. Ukadgaonker and D. K. N. Rao, "A general solution for stresses around holes in symmetric laminates under in-plane loading," *Composite Structure,* vol. 49, pp. 339-354, 2000.

[5] V. G. Ukadgaonker and D. K. N. Rao, "Stress distribution around triangular holes in anisotropic plates," *Composite Structure,* vol. 45, pp. 171-183, 1999.

[6] V.G. Ukadgaonker and V. Kakhandki, "Stress analysis for an orthotropic plate with an irregular shaped hole for different in-plane loading conditions-part-I." *Composite Structure*, vol. 70, pp. 255-274, 2005.

[7] D. K. Nageswara Rao, M. Ramesh Babu, K. Raja Narender Reddy and D. Sunil, "Stress around square and rectangular cutouts in symmetric laminates," *Composite Structure,* vol. 92, pp. 2845-2859, 2010.

[8] J. Daoust and S. V. Hoa, "An analytical solution for anisotropic plates containing triangular holes," *Composite Structure,* vol.19, pp. 107-130, 1991.

[9] J. Rezaeepazhand and M. Jafari, "Stress concentration in metallic plates with special shaped cutout," *International Journal of Mechanical Sciences*, vol.52, pp. 96–102, 2010.

[10] D. S. Sharma, "Stress concentration around circular/ elliptical/triangular cutouts in infinite composite plate, " Lecture Notes in Engineering and Computer Science: Proceedings of the World Congress on Engineering 2011, WCE 2011, 6-8 July, 2011, London, U.K., pp. 2626-2631.

[11] X. L. Gao, "A general solution of an infinite elastic plate with an elliptic hole under biaxial loading," *International Journal of Pressure Vessel and Piping,* vol. 67, pp.95–104, 1996.